Vision Research 50 (2010) 936–946

Contents lists available at ScienceDirect

Vision Research

journal homepage: www.elsevier.com/locate/visres

Morphological differences between the eyeballs of nocturnal and diurnal amniotes revisited from optical perspectives of visual environments

Lars Schmitz [a,b,*], Ryosuke Motani [a]

[a] Department of Geology, University of California Davis, Davis, CA 95616, USA
[b] Department of Evolution and Ecology, University of California Davis, Davis, CA 95616, USA

ARTICLE INFO

Article history:
Received 6 March 2009
Received in revised form 6 January 2010

Keywords:
Nocturnal vision
Diurnal vision
Sensitivity
Scleral ring
Eyeball morphology
Amniotes

ABSTRACT

Eyes are expected to be adapted to the physical characteristics of the visual environment, yet previous analyses failed to corroborate this observation. We demonstrate that nocturnal, crepuscular/cathemeral, and diurnal activity patterns occupy distinct areas in morphospace and are identified with high accuracies based on a discriminant analysis of visual performance features. Not only nocturnal and diurnal diel activity patterns are reflected in macroscopic morphology of the eyeball, but also the crepuscular/cathemeral patterns. The eyeball morphology of the latter was believed to be undistinguishable between diurnal and nocturnal types. We show that all three categories can be delineated with high accuracies.

1. Introduction

The camera eyes of terrestrial animals cope with highly variable light environments, largely depending on the diel activity patterns of the organism. The natural irradiance levels in terrestrial environments span 8–9 orders of magnitude (Land, 1981; Lythgoe, 1979; Martin, 1983). The maintenance of optimal image quality is difficult in low light conditions because the number of photons reaching the retina sets a limit to potential resolution (Charman, 1991). Thus, visually guided animals active in dim-light conditions must enhance visual sensitivity, i.e., the ability to detect weakly illuminated objects by modifying the optical and sensory systems. Every image-forming eye that is optimized for visual sensitivity loses resolving power (Land, 1981). This fundamental trade-off in visual performance involves both optical and sensory mechanisms and is the main reason why contrasting lifestyles, especially diel activity patterns, are reflected in the physiology of the visual system (Warrant, 2008). The optics of the camera eye, i.e., pupil diameter and focal length, define retinal image brightness. Pupil diameter and focal length seem to be closely correlated to gross ocular morphology (Schmitz, 2009). Hence, lifestyles are also expected to affect the overall eyeball shape.

It has long been recognized that eyeball morphology, e.g., gross morphology and retinal structure, and spectral sensitivities of photopigments, reflected the lifestyle of the animal (Land & Nilsson, 2002). The influence of lifestyle on camera eye morphology should be noticeable in all animals that have such eyes, but for comparative purposes it is convenient to focus on groups with similar overall body structure and the possibility to employ a phylogenetic framework for the analysis. In this study we focused on the camera eyes of terrestrial amniotes, including both spherical (Fig. 1a–c) and tubular shape (Fig. 1d). Leuckart (1875) argued that night-active (nocturnal) amniotes tend to have larger eyes than day-active (diurnal) amniotes and recognized the importance of the light-reflective layer in the choroid (*tapetum lucidum*) for improved night vision. He also noticed that nocturnal amniotes, in particular small Rodentia and Carnivora, have relatively thick and strongly curved lenses. Walls (1942) further emphasized the differences between the eyes of nocturnal and diurnal amniotes. He specified that the eyes of the former had larger eyes with larger anterior segment, pupil and lens (Fig. 1a and b).

The disparity between eyes of nocturnal and diurnal amniotes has been repeatedly cited in textbooks (e.g., Duke-Elder, 1958; Prince, 1956; Tansley, 1965) but was never corroborated with morphometric data, despite increased efforts in recent years (e.g. Brooke, Hanley, & Laughlin, 1999; Clement, 2004; Hall, 2008a, 2008b; Hall & Ross, 2007; Kirk, 2004, 2006; Ross & Kirk, 2007; Thomas, Kelly, & Goodship 2004; Thomas, Szekely, Powell, & Cuthill 2006; Thomas et al., 2002; see discussion). It can be concluded from these studies that only extremely nocturnally or diurnally adapted amniote eyes may be clearly identified based on eyeball morphometrics, because there is an overlap between categories of different activity patterns. In particular cathemeral and crepus-

* Corresponding author at: Department of Geology, University of California Davis, Davis, CA 95616, USA.
E-mail address: lschmitz@ucdavis.edu (L. Schmitz).

0042-6989/$ - see front matter © 2010 Elsevier Ltd. All rights reserved.
doi:10.1016/j.visres.2010.03.009

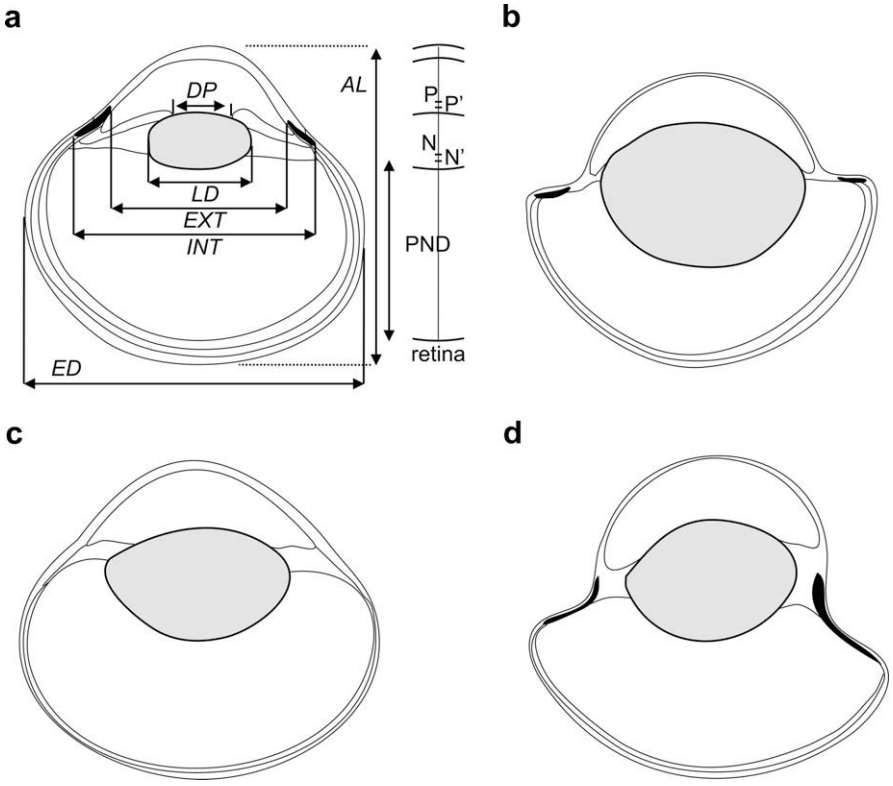

Fig. 1. Generalized cross-sections of terrestrial amniote eyes (not to scale). (a) Eye of a diurnal avian, with explanations of morphological and optical dimensions. (b) Eye of a nocturnal avian with very large lens compared to overall eye size. (c) Eye of a cathemeral mammal. (d) A tubular owl eye with enlarged anterior chamber and steep lateral surfaces of the scleral ring. AL, axial length; DP, diameter of dilated pupil; ED, eyeball diameter; EXT, external scleral ring diameter; INT, internal scleral ring diameter; LD, lens diameter; N, nodal point; N′, posterior nodal point; P, principal point; P′ posterior principal point; PND, posterior nodal distance.

cular amniote eyes fall within the same range as diurnal and nocturnal eyes, and are practically not distinguishable from other categories. The influence of diel activity pattern on eyeball morphology is apparent, yet seems insufficient to result in a clear delineation between the eyes of all different activity patterns. Such a finding is surprising given that the clear distinction between vertebrate eyes with different activity patterns has repeatedly been noted since Leuckart (1875) and Walls (1942) (e.g., Duke-Elder, 1958; Prince, 1956; Tansley, 1965).

If gross morphology of the eyeball were to reflect diel activity patterns, those features that are highly relevant to optical sensitivity should exhibit stronger adaptive signals than those without optical relevance. Then, a morphometric analysis of the optically relevant features may reveal an unambiguous discrimination among different diel activity patterns. The aim of the present work is to test this hypothesis by focusing on the morphometrics of those macro-anatomical features that are strongly correlated with the optics of the eyeball. For example, the lens diameter may be used as a proxy for pupil diameter, the axial length of the eyeball as a proxy for focal length, and the horizontal diameter as proxy for the size of the retina, i.e., the number of photoreceptors. A key aspect of this study is to test if not only nocturnal and diurnal but also cathemeral and crepuscular patterns may be identified based on eyeball morphometrics. The eyes of the latter two categories (Fig. 1c) have been described as intermediate between diurnal and nocturnal (e.g. Hall & Ross, 2007), being practically indistinguishable from either diurnal or nocturnal groups.

1.1. Previous work on the influence of diel activity patterns upon amniote eyeballs

Hughes (1977) pioneered the use of quantitative methods in comparative morphology of vertebrate eyes by employing explicit optical equations to evaluate visual performance. He introduced the light-collection factor, which is the square of the inverse f-number commonly used in optics (e.g., Land, 1981; Martin, 1983). The light-collection factor provides a measure for the brightness of the retinal image (retinal illumination), by approximating the number of photons entering the eye and the size of the projected image. The number of photons largely depends on the size of the aperture, approximately the square of pupil diameter. Retinal image size largely depends on the posterior nodal distance of the refractive system formed by lens and cornea, corresponding to the focal length of an optical system with a single refractive surface. Then, the light-collection factor is given as squared ratio of pupil diameter and posterior nodal distance. Nocturnal vertebrates tend to have relatively higher light-collection factors than diurnal vertebrates, i.e., they project a smaller but brighter image on the retina. However, the ranges of nocturnal and diurnal vertebrates largely overlap (Hughes, 1977; Ross, 2000 [note that Ross (2000) used corneal diameter as a proxy for pupil diameter]). Neither Hughes (1977) nor Ross (2000) attempted to distinguish the eyes of cathemeral (referred to as arrhythmic by Hughes) or crepuscular vertebrates from those of diurnal and nocturnal species.

The last decade has seen a renaissance in the field of comparative eyeball morphology, especially in understanding the ecomorphological significance of primate and avian eyeball morphology. Several investigators analyzed differences between eyes of nocturnal and diurnal amniote eyes (Brooke et al., 1999; Clement, 2004; Hall, 2008a, 2008b; Hall & Ross, 2007; Kirk, 2004, 2006; Ross & Kirk, 2007; Thomas et al., 2002, 2004, 2006). A clear delineation between the eyes of amniotes with different diel activity pattern has yet to be discerned, although evidence is beginning to emerge.

Previous approaches focused on the analysis of morphological features that represent an estimate for *f*-number (aperture/poster-

ior nodal distance). Hall and Ross (2007) and Hall (2008a, 2008b) analyzed dimensions of cornea and axial length as proxies for aperture and posterior nodal distance, respectively. They demonstrated that relative proportions of corneal diameter and axial length are indeed influenced by diel activity pattern among birds and lizards, i.e., statistical differences between the means and/or regressions of the respective groups. However, this does not mean that all members of the groups can be clearly delineated from each other, which is apparent when looking at the bivariate scatter plots. Two variables alone are insufficient to clearly delineate nocturnal from diurnal species, because their respective ranges widely overlap in bivariate morphospace. For example, for a given eyeball morphology, an eye could be either classified as diurnal or nocturnal. Hall and Ross (2007) also attempted to distinguish cathemeral and crepuscular species from diurnal and nocturnal species. However, the former were not statistically different from diurnal species, and the respective ranges of all categories overlapped widely.

Hall (2008b) examined if different activity patterns are reflected in skeletal anatomy, i.e., scleral rings and orbit. She found that nocturnal birds tend to have a larger internal scleral ring diameter for given orbit depth and maximum scleral ring length, yet again, the ranges of both groups overlap widely. Thus, a clear delineation between those two categories was impossible, even though no cathemeral or crepuscular species were included in this study, making a distinction between the other categories easier. Furthermore, the optical significance of scleral ring length, which may be better described as scleral ring height in side view, is unclear. This is problematic in that it is not clear how this variable relates to optical function of the eye, i.e., how the scleral ring length influences retinal illumination.

Kirk (2004) followed a different approach. He analyzed the size of the cornea for a given eyeball diameter in primates and found that nocturnal species tend to have relatively larger corneas. In fact, Kirk (2004) was able to demonstrate that within haplorhine primates and strepsirrhine primates alone the ranges of diurnal and nocturnal species did not overlap. However, when analyzing data from both clades, a clear distinction of nocturnal from diurnal species was not discernable. Hence, an unambiguous discrimination among different diel activity patterns seemed impossible.

2. Materials and methods

2.1. Classification of diel activity pattern

Terrestrial amniotes have different patterns of activity during the daily cycle. We used four different categories that describe the diversity of observed diel activity patterns well: nocturnal, crepuscular, cathemeral, and diurnal. We classified amniotes into these categories based on their peak foraging activities, based on an extensive review of the literature, including primary literature and fully-referenced books. Additionally, we supplemented this information with first-hand observations from experts in the field (Supplementary Tables A1–3). We considered species nocturnal if their foraging activity began at dusk or later and ended not after dawn. Some nocturnal species have two phases of activity during the night, whereas other species show constant levels of activity throughout the night. Please note that both types of nocturnal activity (bimodal and unimodal) expose the organisms to the same light levels. We considered cathemeral species to be active both night and day. For example, we classified a species into the cathemeral group if it had a uni- or bimodal activity pattern with the activity periods ranging from full day-light conditions to low light levels after dusk. We also included species that have a pronounced seasonal variation of main activity (e.g., diurnal in winter, nocturnal in summer) into this group. Similar to the cathemeral species that are active both day and night during one diel cycle, their eyes need to be able to function at both photopic and scotopic conditions. We classified species as crepuscular if they were foraging exclusively at dusk and dawn, during twilight conditions. Based on this definition, one could consider crepuscular activity as a very specialized kind of cathemerality with bimodal activity peaks. Finally, we considered species diurnal if their foraging activity commenced not before dawn and ended at dusk. Similarly to the other categories, some diurnal species have a bimodal activity pattern. However, the light levels experienced by diurnal species with uni- or bimodal activity pattern are equivalent.

We grouped crepuscular and cathemeral amniotes together, because their eyes are expected to have similar light-gathering capacity: crepuscular eyes need to function at intermediate light levels, cathemeral eyes need to function in bright as well as dim light, which should be solved by a compromise between the two extremes.

2.2. Selection of taxa

We measured eyeball soft-tissue dimensions of 66 terrestrial amniote species (37 mammal, 19 bird, and 10 squamate species; $n = 72$) to analyze the correspondence between the diel activity pattern and eyeball shape. Literature-based data form only a small part of the dataset (20 of 66 species). Mammalian, avian, and squamate species that we sampled span 14, 14 and 6 families, respectively (Table A1).

Additionally, we measured osteological dimensions concerning the eyeball: orbit length, the distance from most anterior to most posterior point on the orbit margin, and the external and internal scleral ring diameters. Measurements were taken from 77 terrestrial avian species ($n = 98$), spanning 30 families (Table A2). Lastly, we measured external and internal diameters of isolated scleral rings from 251 additional terrestrial avian species ($n = 1499$) across 60 families (Table A3).

Amniotes usually have spherical eyes but there are exceptional cases where the eyeballs are tubular, as in owls. Both shapes are represented in our taxonomic sampling of soft-tissue and osteologic data.

2.3. Soft-tissue dimensions

Eyeballs are very fragile structures, and their dimensions may change quickly *post mortem*, depending on the use of fixatives. This does not necessarily concern eyeball axial length and equatorial diameter, but lens and possibly corneal dimensions (Augusteyn, Rosen, Borja, Ziebarth, & Parel, 2006). A major problem is a volume gain of the lens, which is primarily caused by an increase of an average 8.7% ($n = 10$) in lens thickness through water intake (Augusteyn et al., 2006).

We measured soft-tissue dimensions from paraffin embedded eyes in the collections of the Zoological Society of the San Diego Zoo. The following procedures were adopted by the Zoo staff in making these sections. Eyes were excised within a maximum of one day after death of the animal and then immediately fixed in Davidson's solution. The eyes were refrigerated, which minimizes lens cracking due to volume change by swelling and freezing. The eyeball was then hemi-sectioned sagittally and routinely embedded in paraffin. Eyes who appeared deformed due to loss of intraocular pressure after removal were not used for this study. Furthermore, all sections were observed with a binocular microscope to examine the accuracy of the position of hemi-sections, using the clear crystalline lens and the iris as point of reference. Measurements were taken from digital photographs. A Nikon D70 with a Nikon AF Micro Nikkor 60 mm lens was used. Additional data on eyeball soft-tissue dimensions were retrieved from

published schematic eyes, frozen specimens, and morphological descriptions (Table A1).

2.4. Macro-anatomical correlates of optical parameters

Posterior nodal distance (PND), the distance from the posterior nodal point to the retina surface, and the diameter of the fully dilated pupil (DP) are the two main optical parameters of the amniote eye (Fig. 1a and b). Because published data of both PND and DP are only available for a limited number of species, we needed morphological proxies for these optical variables (Fig. 1a). Several authors demonstrated that PND is correlated with eyeball axial length (Hughes, 1977; Murphy & Howland, 1987; Pettigrew, Dreher, Hopkins, McCall, & Brown, 1988; Schmitz, 2009), and the diameter of DP is correlated with equatorial lens diameter (Hughes, 1977; Schmitz, 2009).

2.5. Regularized and quadratic discriminant analyses

We performed regularized and quadratic discriminant analysis (RDA and QDA, respectively) on eyeball soft-tissue dimensions (diameter, axial length, lens diameter) and osteological dimensions (orbit length, axial length, and lens diameter) with the klaR and MASS package on the software platform R 2.8.0. We transformed all measurements into logarithms (base 10) before the analysis, which accounts for the effect that residuals tend to become larger for larger variables. Discriminant analysis entails the derivation of a variate (“discriminant function”), which results from linear combinations of those independent variables that most accurately discriminate between groups (Friedmann, 1989). The classification of observations follows according to classification functions, which use the distance between discriminant scores and group centroids to calculate probabilities to which group each observation most likely belongs to (Friedmann, 1989). Diverse discriminant methods mostly differ from each other in the way they estimate variances and covariances. Linear discriminant analysis uses pooled covariance of variables, thus assuming a uniform covariance across the groups being analyzed, whereas quadratic discriminant analysis uses covariances of each group, assuming unequal covariances. Neither of these special cases is likely to occur in biometric datasets, and thus we used RDA, which is a compromise between linear and quadratic discriminant analyses (Friedmann, 1989). We set the two regularization parameters λ and γ to 0.05 and 0, respectively, to minimize the risk of misclassification. A λ of 0.05 and γ of 0 are very close to a quadratic discriminant analysis, and indeed a Box's *M*-test indicates heterogeneity of the covariances ($p < 0.0001$). However, Box's *M*-test is known to be sensitive to unequal group size, and even a very small *p*-value may erroneously suggest heterogeneity (Rencher, 2002). Importantly, RDA with small λ and $\gamma = 0$ and QDA yielded similar results.

2.6. Test for phylogenetic effects

We calculated the *K*-statistic of Blomberg, Garland, and Ives (2003) to investigate the strength of phylogenetic bias in our data (Tables 1 and 2). We reconstructed two tree topologies for the taxa in our data, namely for all amniotes (Fig. 2) and only for avians (Fig. 3) based on Donne-Goussé, Laudet, and Hänni (2002), Schulte, Valladares, and Larson (2003), Vidal and Hedges (2005), Ericson et al. (2006), Bininda-Emonds et al. (2007), Marcot (2007), and Hackett et al. (2008). We performed the calculation of *K*-statistics with the picante package on the software platform R 2.8.0.

Branch length estimates were largely unavailable for each tree. We accounted for this problem in two different ways. First, we used the software Mesquite (Maddison & Maddison, 2008) to derive four different arbitrary branch length models, namely all-equal, Grafen, Nee, and Pagel models. The Grafen model assumes that tips are contemporaneous. The depth of each node equals number of species in the clade defined by the node minus one. Branch length from the tips to the current node modeled by the Nee model is given as the distance equal to the logarithm (base 10) of the number of tips descending from that node. Pagel's model assumes that all internodes have a length of one, and all tips are contemporaneous. Second, we used divergence age of the major clades (Bininda-Emonds et al., 2007; Ericson et al., 2006; Pereira & Baker, 2006; Slack et al., 2006; Vidal & Hedges 2005) to estimate an ultrametric tree for amniotes and avians in our study (Figs. A1 and A2). There is discrepancy in divergence age of avian clades between Pereira and Baker (2006) and Slack et al. (2006). The discrepancy is largest for the split between Palaeognathae/Neognathae and Galloanserae/Neoaves. In order to account for this problem, we built two different ultrametric trees (Figs. A1 and A2). The results were very similar, and thus we show only the trees with node estimates following Pereira and Baker (2006).

Divergence ages for many higher nodes (e.g., within the Bovidae) were not available. Thus, we assumed equal internode length in these clades, with all tips being contemporaneous. In order to validate this approach, we compared the estimated divergence ages with the fossil record of mammalian (McKenna & Bell, 1997) and avian (Mayr 2005) families, and found the results to be largely consistent.

Table 1
Test for Adequate standardization of data.

Branch length model	*p*-value			
	ED	AL	LD	LD^2/ED * AL
Amniotes				
All 1	0.1603	0.0512	0.0233	0.0439
Grafen	0.0079	0.0037	0.0005	0.002
Nee	0.4382	0.1821	0.0457	0.0852
Pagel	0.0147	0.0049	0.0006	0.0075
Ultrametric estimate 1	0.589	0.3269	0.1367	0.168
Branch length model	OL	EXT	INT	INT^2/OL * EXT
Avians				
All1	0.3996	0.0915	0.1059	0.2512
Grafen	0.0064	0.0007	0.0017	0.0121
Nee	0.5125	0.0579	0.1573	0.1279
Pagel	0.1294	0.0198	0.0351	0.1029
Ultrametric estimate 1	0.5725	0.9802	0.9224	0.2897

Tree topology is based on Fig. 2 (amniotes) and Fig. 3 (avians). Divergence ages for ultrametric trees are provided in Figs. A1 and A2. *P*-values are given for a *F*-test whether the slope of the regression line of absolute standardized contrast plotted against their standard deviations is different from zero. Only the ultrametric models (amniotes and avians), Nee-model (avians), and the all1-model (avians) adequately standardize the data.

Table 2
Test for phylogenetic effect.

Branch length model	Blomberg's *K*			
	ED	AL	LD	LD^2/ED * AL
Amniotes				
Ultrametric estimate 1	1.0145	0.9922	0.8297	0.3741
Branch length model	OL	EXT	INT	INT^2/OL * EXT
Avians				
All1	0.8731	0.7861	0.8143	0.3868
Ultrametric estimate 1	1.0983	0.8434	0.8545	0.4357
Nee	1.0726	1.0473	1.0139	0.7733

Tree topology is based on Fig. 2 (amniotes) and Fig. 3 (avians). Branch lengths for ultrametric trees are provided in Figs. A1 and A2. Only branch length models that adequately standardize the data (see Table 1) were included in this test.

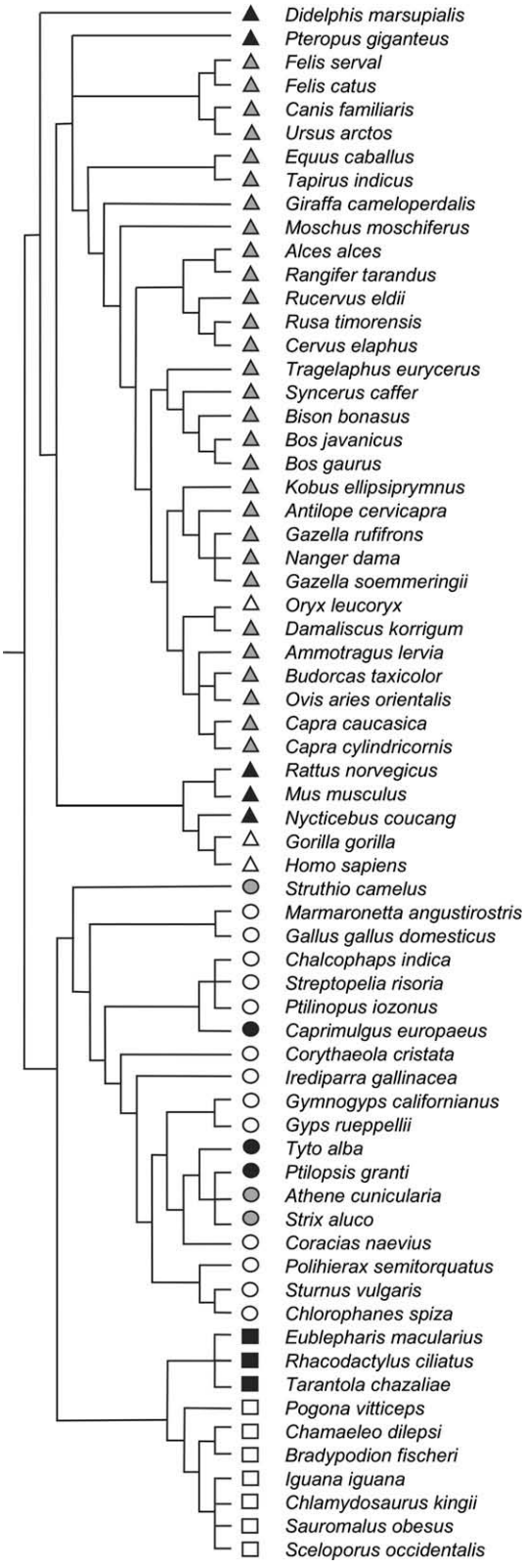

Fig. 2. Phylogenetic relationships and distribution of diel activity pattern of amniotes analyzed in this study. Tree topology is based on Donne-Goussé et al. (2002), Schulte et al. (2003), Vidal and Hedges (2005), Ericson et al. (2006), Beninda-Emonds et al. (2007), Marcot (2007), and Hackett et al. (2008). Circles represent avians, triangles represent mammals, and squares indicate squamates. Black fillings identify nocturnal species, and grey fillings identify cathemeral and crepuscular species. Open symbols represent diurnal species.

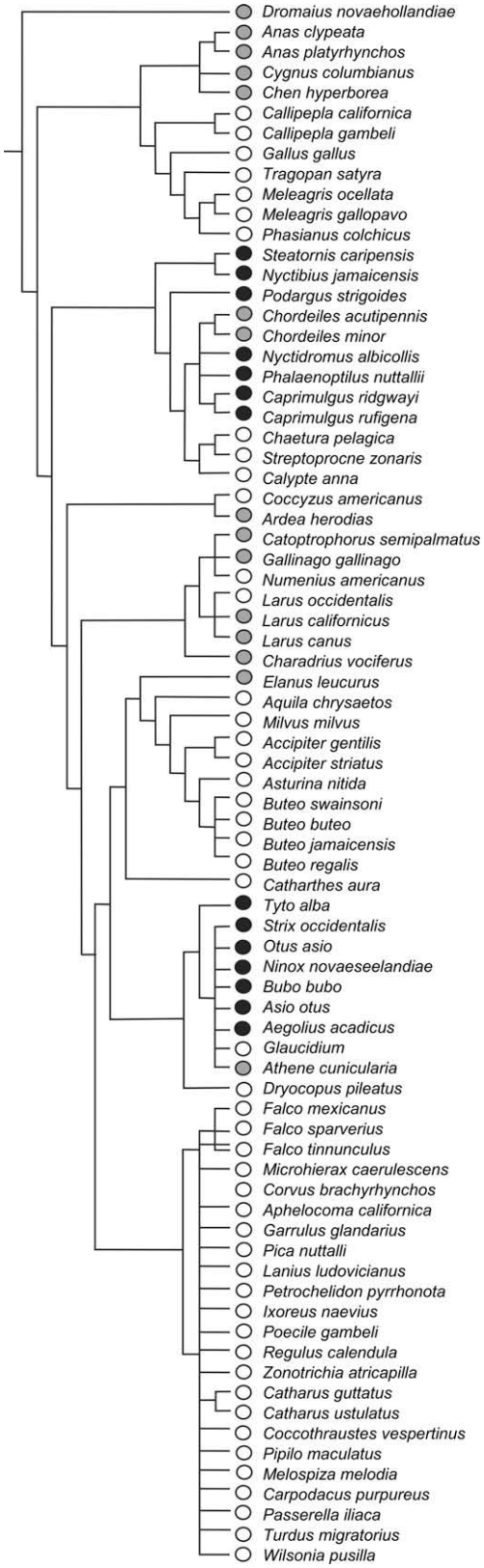

Fig. 3. Phylogenetic relationships and distribution of diel activity pattern of avians analyzed in this study. Tree topology is based on Donne-Goussé et al. (2002), Ericson et al. (2006), and Hackett et al. (2008). Black circles identify nocturnal species, and grey fillings identify cathemeral and crepuscular species. Open circles represent diurnal species.

We tested whether the branch lengths adequately fit the tip data (Garland, Harvey, & Ives 1992; Diaz-Uriarte & Garland 1996, 1998; Garland, Midford, & Ives, 1999) using different models available in the PDAP package of Mesquite (Midford et al., 2003). We plotted absolute standardized phylogenetically independent contrasts of each variable against their standard deviations, and tested if the slope of the least-square regression line differs from zero (Table 1). The branch length model appropriately standardizes the data if the slope is not different from zero.

3. Eyeball morphology and diel activity pattern

3.1. Physiological optics and light sensitivity

Physiological optics predicts several modifications of the optical system of amniote eyes that would increase light-gathering capacity. Land's sensitivity equation (Land, 1981) provides an anatomical model for visual sensitivity to extended light sources, and combines optical parameters and retinal characteristics. Inferred by optics alone, i.e. without considering retinal characteristics, visual sensitivity to extended light sources increases proportional to retinal illumination (RI), given by DP^2/PND^2 (Hughes, 1977; Land, 1981). DP is the diameter of the fully dilated pupil, and PND is the posterior nodal distance. A large value for RI corresponds to a low value for the commonly used *f*-number in optics, the inverse square root of RI. The anatomical model for visual light sensitivity to point light sources, such as stars and bioluminescent flashes, optically depends on DP^2 (Land, 1981; Warrant, 2004).

Both optical and anatomical light sensitivities are not performance measures of visual capacity, but they strongly indicate behavioral light sensitivity. Amniote eyes that are optimized for high RI tend to have sensory adaptations suited for dim-light conditions. For example, eyes with low minimum *f*-number have a retina densely packed with rods, which sometimes are arranged in multiple layers (Martin, Rojas, Ramirez, & McNeil, 2004), and high summation of rod inputs at ganglion cells. Furthermore, a low minimum *f*-number seems to be correlated with a low absolute visual threshold (Martin, 1983).

3.2. Hypothesis and test

Based on physiological optics, an amniote eye that is adapted to a dim light environment is expected to have: (1) a large DP compared to PND to increase retinal image brightness; and (2) a large DP compared to eyeball diameter (ED) to maximize the number of photons entering the eye (proportional to DP), for a given number of photoreceptors (assumed proportional to ED) and summation of photoreceptor input at ganglion cells. The larger the ratio DP/ED, the greater the likelihood of detecting a visual signal and the brighter the retinal image, provided PND remains constant. Because both ratios contribute to visual light sensitivity of the eye, we combined (1) and (2) and hypothesized that nocturnal amniotes have a larger DP^2 for given ED $*$ PND than crepuscular/cathemeral and diurnal amniotes. Physiological optics predicts that in the bivariate plot of these two variables, eyes of equal light-gathering capacity should plot along the same line with a slope of one.

We plotted the square of lens diameter (as a proxy for DP) versus the product of eyeball diameter and axial length (as proxies for ED and PND, respectively), and grouped amniotes according to their diel activity patterns (Fig. 4a). The plot confirms our hypothesis that nocturnal amniotes have a larger DP^2 for given ED $*$ PND than crepuscular/cathemeral and diurnal amniotes. Importantly, nocturnal amniotes are fully delineated from diurnal amniotes among species with spherical eyes. Amniotes with tubular eye shape (primates, owls) blur the distinction, i.e., the nocturnal owl

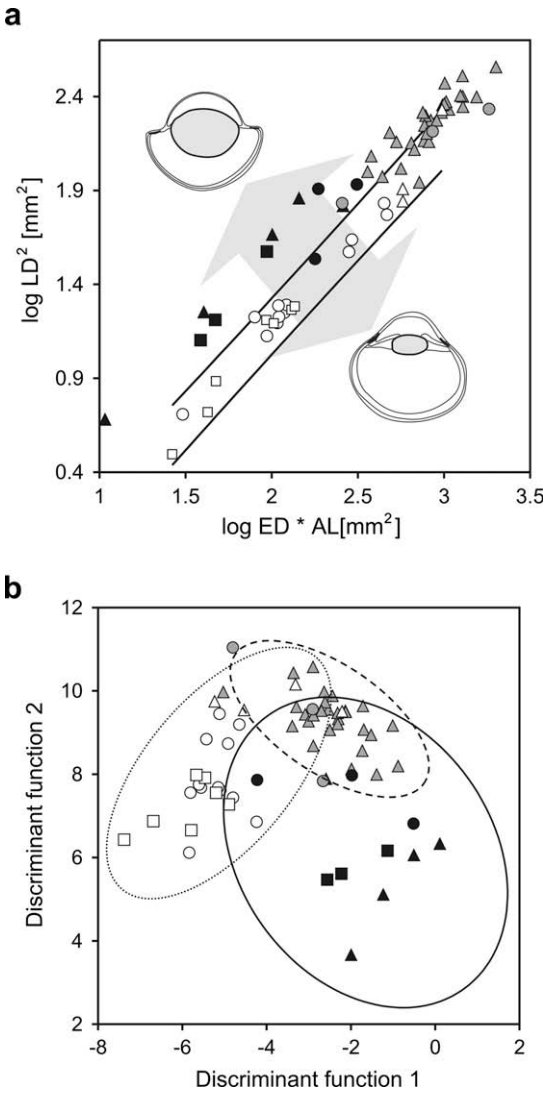

Fig. 4. (a) Plot of the square of lens diameter versus the product of eyeball diameter and axial length of terrestrial amniotes. Nocturnal amniotes plot above the 95% prediction belts calculated for diurnal amniotes. (b) Plot of discriminant functions (DF) 1 and 2 found by RDA of eyeball diameter (ED), axial length (AL), and lens diameter (LD) of terrestrial amniotes. Circles represent avians, triangles represent mammals, and squares indicate squamates. Black fillings identify nocturnal species, and grey fillings identify cathemeral and crepuscular species. Open symbols represent diurnal species. For each group of activity pattern 95% confidence ellipses are plotted.

Ptilopsis granti is within the range of diurnal taxa. Crepuscular and cathemeral amniotes plot intermediate to nocturnal and diurnal amniotes at the very large end of the range, as we expected based on their visual environments. We cannot clearly distinguish crepuscular/cathemeral amniotes from other amniotes on the basis of these measurements alone, because they overlap widely. Thus, we performed a RDA on optically significant parameters (LD, ED, AL) to explore if it is possible to achieve a better discrimination.

RDA almost completely discriminates crepuscular/cathemeral amniotes from diurnal and nocturnal amniotes (Fig. 4b). The method classified 95.08% of all species to their correct diel activity pattern in our sample of spherical eye shape ($n = 61$), and 90.91% in our sample of both spherical and tubular eye shapes ($n = 66$). Among species with spherical eye shape, erroneous classification only occurred between crepuscular/cathemeral and diurnal species. When we included tubular eyes in the analysis, the nocturnal owl *Ptilopsis granti* was misclassified as diurnal.

Both discriminant functions are variations from the optically derived ratio, $DP^2/ED * PND$. Discriminant function 1 is formed by positive loading of LD (+19.9) and negative loadings of ED and AL (−10.8 and −6.3, respectively); discriminant function two is formed by positive loadings of AL and ED (5.7 and 5.4, respectively) and negative loading of LD (−6.2). The loadings are the coefficients of the variables (ED, AL, LD) of the discriminant functions.

We also investigated if osteological features of the eye and orbit are useful in discriminating avians of different diel activity patterns. Ossifications within the eye, namely scleral ossicles, are widespread among vertebrates, and are probably secondarily lost in snakes, mammals, crocodiles, and most extant amphibians (Edinger, 1929; Franz–Odendaal & Hall, 2006). Whereas the number of scleral ossicles varies greatly among amniotes (Edinger, 1929; Franz-Odendaal & Hall, 2006) their position at the cornea-sclera junction remains unchanged. The scleral ossicles form an imbricate ring (scleral ring), which encloses an elliptical to circular opening that leaves space for lens and pupil (Fig. 6a).

Ossification in the eyeball of amniotes (scleral rings) and the eye socket in the skull (orbit) are often regarded to reflect the shape and size of the eye (e.g. Brooke et al., 1999; Edinger, 1929; Motani, Rothschild, & Wahl, 1999), and indeed, recent studies found quantitative evidence (Hall, 2008b; Schmitz, 2009). For example, the lens diameter (LD) scales isometrically to the internal diameter of the scleral ring (INT): $LD = 0.7INT$ ($r^2 = 0.95$) (Schmitz, 2009). The eyeball diameter (ED) is correlated to the external diameter of the scleral ring (EXT): $ED = 1.88EXT^{0.84}$ ($r^2 = 0.97$). Eyeball axial length (AL) can also be estimated from EXT, because ED and AL are highly correlated among birds: $AL = 1.06ED^{0.93}$ ($r^2 = 0.97$). This strong correlation allows for calculation of eyeball axial length as $AL = 2EXT^{0.78}$. Finally, orbit length (OL) is another proxy for ED: $ED = 1.34OL^{0.87}$ ($r^2 = 0.95$).

We tested if the dimensions of the scleral ring alone contain the information necessary to clearly distinguish groups of different activity pattern. The scaling equations provided above offer the possibility to calculate eyeball soft-tissue dimensions from scleral rings, including eyeball diameter, axial length, and lens diameter. We thus tried to estimate these dimensions from scleral ring measurements of terrestrial birds ($n = 252$). However, when plotting the birds onto the DA space based on soft-tissue dimensions, a clear bias surfaced (Fig. 5a): large animals with large eyes tended to be erroneously classified as nocturnal, and small animals with small eyes as diurnal; note that discriminant function 2 is strongly positively correlated with size (Fig. 5b). The bias ultimately shows that the two measurements (INT and EXT) cannot account for the information contained in three measurements (LD, ED, and AL) that are necessary for the correct classification that we established in the previous section. Indeed, when plotting INT versus EXT (Fig. 6a), the discrimination among different diel activity patterns is not as clear.

We accounted for this bias by adding another measurement, namely OL, and thus building a new DA space based on OL, EXT, and INT. The scatter plot of discriminant scores of this new space is unbiased (Fig. 6b), and yielded a reasonable discrimination of groups with different activity pattern −85.3% of our sampled taxa with spherical eyes ($n = 68$, Table A2) were correctly classified according to their diel activity patterns, using QDA. QDA of taxa with both spherical and tubular eye shape yielded a correct classification of 83.1% ($n = 77$).

4. Discussion

We present the first quantitative method to discriminate among diurnal, crepuscular/cathemeral, and nocturnal amniotes based on eyeball morphometrics with high accuracies. It confirms an early generalization by Leuckart (1875) and Walls (1942) that diel activity patterns are so strongly reflected in the morphometrics of the eyeball that eyeballs of different light-level adaptations are fundamentally different from each other. Our approach differs from many previous studies in that we combine morphometric data from a wide range of terrestrial vertebrates, including mammals, avians, and squamates that have comparable overall eye morphology. The success of our method is mainly attributable to the selection of morphometric features based on the predictions from optics, and the application of discriminate analysis.

The largest conceptual advance of our contribution is that we can delineate cathemeral/crepuscular species from other groups, in contrast to previous studies. Figures in numerous studies (e.g., Hall & Ross, 2007) show that cathemeral and crepuscular species

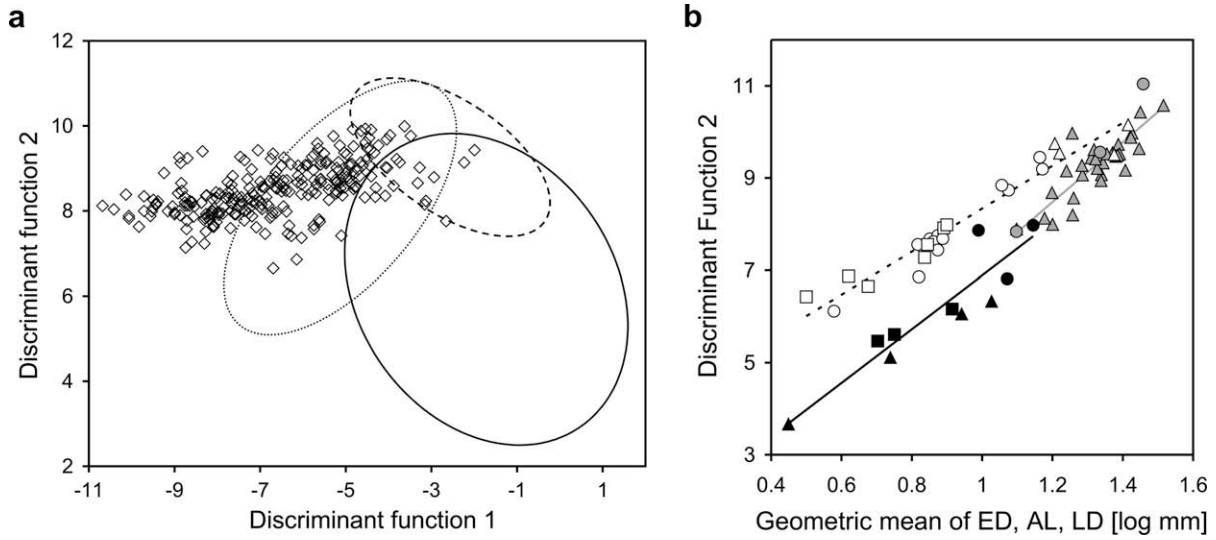

Fig. 5. (a) A plot of discriminant scores (open diamonds) of estimated ED, AL, and LD based on scleral ring dimensions of extant birds onto the original, soft-tissue defined RDA space. The scatter of discriminant scores is clearly biased. (b) A plot of DF 2 (based on soft-tissues) versus the geometric mean of ED, AL, and LD, showing a positive correlation of DF 2 with eye size. Lines represent RMA regression lines. Circles represent avians, triangles represent mammals, and squares indicate squamates. Black fillings identify nocturnal species, and grey fillings identify cathemeral and crepuscular species. Open symbols represent diurnal species.

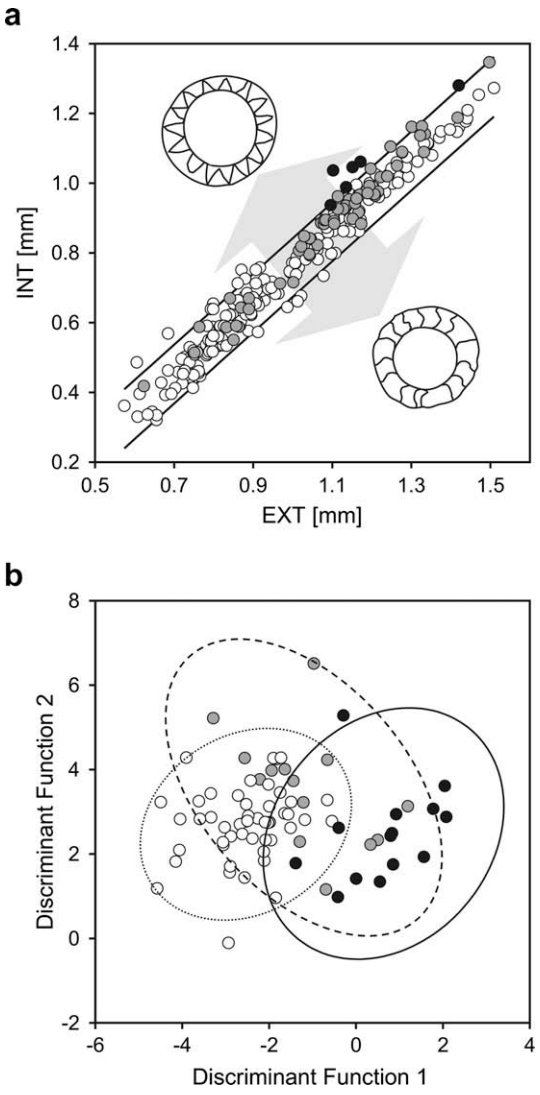

Fig. 6. (a) Plot of the internal scleral ring diameter (INT) versus the external scleral ring diameter (EXT) of terrestrial avians. Nocturnal species tend to have a larger INT for given EXT than diurnal and cathemeral/crepuscular species, yet their respective ranges widely overlap. (b) Plot of DF 1 and 2 found by QDA of orbit length, external and internal scleral ring diameter. Black fillings identify nocturnal species, and grey fillings identify cathemeral and crepuscular species. Open symbols represent diurnal species. For each group of activity pattern 95% confidence ellipses are plotted.

plot within the wide area of overlap between diurnal and nocturnal species. This overlap pertains also after removal of tubular eye shapes that we did not include in our analysis (see below). Thus, cathemeral and crepuscular species seemed indistinguishable from other groups. The bivariate plot that we derived based on two optical ratios minimizes the range of overlap. However, this plot is still clearly insufficient to distinguish cathemeral and crepuscular from diurnal and nocturnal groups, similar to previous studies (e.g., Hall & Ross, 2007). Discriminant analysis delineates all three different groups with high accuracy. Importantly, the discriminant axes of this analysis are modifications of the optically derived ratio, i.e., the delineation between groups of different activity patterns is directly related to optical sensitivity. The remaining uncertainty in the classification may be due to at least two factors. First, we used morphological proxies to represent underlying optical parameters. The proxies are tightly correlated with the optical variables, yet there is variation, which probably accounts for a part of the uncertainty. Second, additional functional constraints may influence the morphological and functional design of eyes. For example, the ratio of corneal to lens power is related to retinal image size and likely to visual acuity (Ott & Schaeffel 1995). Therefore, organisms with high visual acuity may have smaller and thinner lenses, which could interfere with optimization of light sensitivity.

The distinction between groups of different activity patterns is also achieved with a discriminant analysis of skeletal features of extant avians, which is a major advance compared to a previous study (Hall, 2008b). Even though the analyzed features, namely orbit length and external and internal diameters of the scleral ring, are correlated with visual performance (Schmitz, 2009), the accuracy of resulting classification is inferior to that based on the soft-tissue dataset. This clearly points to additional factors controlling the shape and size of respective osteologic features. These factors may include differences in degree of ossification due to, for example, different demands for mechanical stability of the eye, and interference with other structures of the head. Nevertheless, QDA performed reasonably well in delineating groups of activity patterns.

Hall (2008b), who did not include any cathemeral and crepuscular species, found differences in the regression lines of nocturnal and diurnal avians (Hall, 2008b: Fig. 3); yet the respective ranges of diurnal and nocturnal species widely overlap. Consequently, only extremely nocturnally and diurnally adapted species could be identified based on osteology, whereas the majority of species falls in the range of overlap. Furthermore, it is not necessary to include orbit depth for a reliable interpretation of diel activity pattern with skeletal features, contrary to a previous perception (Hall, 2008b). Orbit depth is difficult to measure even if there is a complete skull. The method we present here has great potentials for the inference of diel activity pattern of extinct avians. The osteological features needed for this analysis, OL, EXT, and INT are readily available in a large number of fossil species, and thus one can derive a reliable estimate of the diel activity pattern. Such a paleontological analysis is beyond the scope of the present contribution but would enhance our understanding of the evolution of this trait among basal avians.

It has been argued that interspecific biometric datasets do not contain statistically independent samples because of the hierarchical phylogenetic system (Felsenstein, 1985). Different diel activity patterns are well represented in the sampled amniotes (Fig. 2). Nocturnal and diurnal species are present in mammals, avians, and squamates, cathemeral/crepuscular species in mammals and avians. A possible phylogenetic bias might arise in the analysis of avians, because all sampled nocturnal species fall within two clades (Caprimulgiformes + Apodiformes; Strigiformes; see Fig. 3). However, diurnal and crepuscular/cathemeral species are widely distributed and are present in all major clades (Palaeognathae, Galloanserae, and Neoaves).

First, we tested if the branch length models adequately standardize the observed tip data for statistical purposes (Table 1). None of the branch length models fulfill this criterion for the given tree topology of the amniote phylogeny, except the ultrametric estimate of branch length ($p > 0.05$). The slopes of the least-square regression line of the phylogenetically independent contrasts (PIC) of all other variables and branch length models plotted against their standard deviations are different from zero. We found a similar result when testing the avian phylogeny. Only the ultrametric, all1, and Nee-model seem to appropriately standardize the data. The slopes of the regression lines for IC of OL, EXT, INT, and the ratio $INT^2/AL * EXT$ plotted against their standard deviations are different from zero when using the Grafen- and Pagel-model. Hence, we only used the following branch length models and variables for the calculation of Blomberg's *K*-statistic: ultrametric estimate for amniote phylogeny; ultrametric estimate, Nee-, and all1-model for the avian phylogeny.

We tested how the individual morphological variables and the optical ratio $LD^2/ED * AL$, which best distinguishes between eyes

of amniotes with different activity patterns, relates to phylogeny. We used the *K*-statistic of Blomberg et al. (2003) to estimate the strength of the phylogenetic signal. *K* of less than one implied that close relatives are less similar than expected for given tree topology, branch length, and assumed Brownian motion of evolutionary change. The deviation from Brownian motion indicated that the analyzed character is possibly adaptive, provided the used phylogeny is appropriate (Blomberg et al., 2003).

Next, we calculated *K*-values for all soft-tissue variables and the optical ratio based on soft-tissue dimensions among amniotes ($LD^2/ED * AL$). The *K*-values of ED, AL, and LD were close to one (Table 2). This result is not surprising, given that eye size scales with body size (Howland, Merola, & Basarab, 2004; Ritland, 1982). Body size is liable for phylogenetic bias (e.g., Blomberg et al., 2003). However, we discriminate between activity patterns on an optically derived ratio ($LD^2/ED * AL$). This ratio is independent of body size and has a *K*-value of far less than one (0.3741, Table 2). This strongly indicates that the optical ratio tends to be homoplastic. Then, we calculated *K* for all osteological features and the osteological equivalent of the optical ratio, namely $INT^2/OL * EXT$. Again, most *K*-values of individual features were close to one (Table 2). However, the osteological equivalent of the optical ratio has *K*-values of far less than one (<0.5 for both ultrametric and all1-model). Given that the phylogenetic bias on the optical ratio is small, we did not use the method of PIC (Felsenstein, 1985) or generalized least-squares (GLS; Grafen, 1989). Moreover, there currently is no established method to implement IC in discriminant analyses, whereas the GLS method, as currently implemented, does not accommodate additional categorical variables.

The inclusion of owls and a nocturnal primate partially compromised the classification of diel activity patterns, i.e., the proportion of correctly classified taxa in our samples decreased from 95.02% to 90.91%. Both owls and nocturnal primates have a peculiar eye shape, which is often referred to as tubular (Castenholz,1984; Charman, 1991; Martin, 1982; Walls, 1942; Fig. 1d), and may represent a different evolutionary pathway to increase light-gathering power. The decisive difference is that the lens of owls and nocturnal primates is unusually small compared to other nocturnal amniotes, and with long anterior and posterior radii of curvature. We assume that the tubular eye shape of nocturnal primates and owls leads to violation of two of our original assumptions. First, we used lens diameter as a proxy for the maximum entrance pupil diameter. The relatively small lens compared to other nocturnal amniotes may suggest that the refractive power of the cornea is proportionally larger than in spherical eye types. A relatively higher magnification of the cornea will increase the diameter of the maximum entrance pupil diameter. Consequently, lens diameter is likely to underestimate the size of the entrance pupil diameter, which in turn will cause an underestimate of light-gathering power.

Second, we used eyeball diameter as a proxy for the size of the retinal area and the number of photoreceptors. The retina covers the vitread part of the posterior segment and usually covers the entire area towards the junction of sclera and cornea. However, tubular eyes may be different in this aspect. It has been observed for owls that the retina does not cover the parts of the posterior segment that are vitread to the steep and large scleral rings (Martin, 1982; personal observation, LS). The retina of owls likely does not extend towards the junction of sclera and cornea. Hence, the retinal area for given eyeball diameter is likely smaller in the tubular eye type, which again would cause an underestimate of light-gathering power.

Unfortunately, there are no data currently available to test these hypotheses. There are only two detailed analyses of the schematic eye of an owl (Martin, 1982; Schaeffel & Wagner, 1996). In order to test for differences between the diameters of lens and maximum entrance pupil diameter more comparative data from both the tubular and spherical eye type are needed. Similarly, more data are needed to test for differences between the proportion of eyeball diameter and retinal area. This study should be accompanied by an analysis of the scaling of the number of photoreceptor and ganglion cells with eyeball diameter, as well. Such analyses are beyond the scope of the present contribution but would enhance our understanding of tubular and spherical eye types and their comparative optics.

Our approach is applicable to the very large majority of all terrestrial amniote species. Only nocturnal primates and owls, both of which have distinct eyeball morphologies, are difficult to interpret in respect to their diel activity pattern. Together, nocturnal primates and owls account for far less than 5% of all amniote species. Our analysis is applicable with very high reliability (95%) to many different cathemeral and nocturnal terrestrial amniotes, e.g., geckos, nightjars and allies, ducks, herons, shorebirds, not to mention the large number of many nocturnally and cathemerally active mammals. Nevertheless it is desirable to develop methods that render it possible to include all amniotes. However, this is currently hampered by the unavailability of schematic eye data, which are necessary to re-adjust the morphological proxies for entrance pupil diameter, the number of photoreceptors, and the summation of photoreceptor input at ganglion cells.

A potential problem arises if there is a need to infer the diel activity pattern of an unknown bird based on osteological measurements. Fortunately, the fundamental differences in ocular structure of tubular and spherical eyes are also apparent in scleral ring morphology, which is characterized by very steep lateral surfaces (Fig. 1d). Therefore, it is possible to exclude tubular eyes based on scleral ring morphology alone.

5. Summary

To conclude, the key to an unambiguous discrimination of different diel activity patterns with eyeball morphology is to focus on macroscopic features that have known optical implications. Physiological optics provides the tool to formulate hypotheses on light-gathering capacity of eyes, and ideally one would test these hypotheses with original optical parameters of schematic eyes. The accuracy of morphometric analyses improves with increasing data size, yet schematic eye data for amniotes are limited. However, it is possible to use morphological features as proxies for these optical parameters (Schmitz, 2009), which renders it possible to sample a larger number of taxa. In exploring morphological differences between nocturnally and diurnally adapted amniote eyes, earlier investigators have not fully exploited the predictions from physiological optics. For example, several authors focused on morphological estimates of the *f*-number, which by itself is insufficient to unambiguously identify different activity pattern. The *f*-number is a very valuable descriptor of light-gathering power, yet it does not account for the number of photoreceptors. Additionally, some of the morphological features used have not yet been tested for their optical relevance, e.g., corneal diameter is often assumed to be correlated to dilated pupil diameter, yet a detailed analysis of the scaling relation between these two features is still unavailable. The morphometric analysis we present in this paper is based on optically relevant macroscopic eyeball features with well-known structure–function relationships. We show that it is possible to discriminate different activity patterns, including diurnal, cathemeral/crepuscular, and nocturnal, based on eyeball morphometrics with high accuracy, using predictions from physiological optics.

Acknowledgments

We thank I. and A. Engilis, Museum of Fish and Wildlife Biology of the University of California at Davis, for providing salvaged bird specimens and preparation assistance, and the Zoological Society of San Diego for access to their collection, in particular to R. Papendieck and staff. D. Rimlinger and C. Penny, Zoological Society of the San Diego Zoo provided information on diel activity pattern. C. Cicero, M. Flannery, K. Seymour, and R. van den Elzen granted access to specimens in their collections. S. Price gave valuable suggestions regarding phylogenetic comparative methods. We thank S. Carlson, I. Schwab, G. Vermeij, P. Wainwright, the editor J. Wallman, and three anonymous reviewers for constructive comments. RM discovered that the combination of D/PND and D/L delineated between diurnals and nocturnals, and that RDA discriminated among diel activity patterns unlike LDA. LS was supported by a doctoral stipend of DAAD (German Academic Exchange Service) and by Durrell Funds of the Department of Geology, UC Davis. RM was supported by National Science Foundation EAR 0551024.

Appendix A. Supplementary material

Supplementary data associated with this article can be found, in the online version, at doi:10.1016/j.visres.2010.03.009.

References

Augusteyn, R. C., Rosen, A. M., Borja, D., Ziebarth, N. M., & Parel, J.-M. (2006). Biometry of primate lenses during immersion in preservation media. *Molecular Vision, 12*, 740–747.

Bininda-Emonds, O. R. P., Cardillo, M., Jones, K. E., MacPhee, R. D. E., Beck, R. M. D., Grenyer, R., et al. (2007). The delayed rise of present-day mammals. *Nature, 446*(7135), 507–512.

Blomberg, S. P., Garland, T., Jr., & Ives, A. R. (2003). Testing for phylogenetic signal in comparative data: Behavioural traits are more labile. *Evolution, 57*(4), 717–745.

Brooke, M. D., Hanley, S., & Laughlin, S. B. (1999). The scaling of eye size with body mass in birds. *Proceedings of the Royal Society London Series B, 266*(1417), 405–412.

Castenholz, A. (1984). The eye of Tarsius. In C. Niemitz (Ed.), Biology of Tarsiers (pp. 303–318). Stuttgart, New York: Gustav Fischer–Verlag.

Charman, W. N. (1991). The vertebrate dioptric apparatus. In J. R. Cronly-Dillon & R. L. Gregory (Eds.), *Evolution of the eye and visual system* (pp. 82–117). Boca Raton, Ann Arbor, Boston: CRC Press, Inc.

Clement, R. A. (2004). A quantitative description of lens eye morphology and its implications. *Ophthalmic and Physiological Optics, 24*(3), 242–245.

Díaz-Uriarte, R., & Garland, T. Jr., (1996). Testing hypotheses of correlated evolution using phylogenetically independent contrasts: Sensitivity to deviations from Brownian Motion. *Systematic Biology, 45*(1), 27–47.

Díaz-Uriarte, R., & Garland, T. Jr., (1998). Effects of branch length errors on the performance of phylogenetically independent contrasts. *Systematic Biology, 47*(4), 654–672.

Donne-Goussé, C., Laudet, V., & Hänni, C. (2002). A molecular phylogeny of anseriformes based on mitochondrial DNA analysis. *Molecular Phylogenetics and Evolution, 23*(3), 339–356.

Duke-Elder, S. (1958). *System of ophthalmology: The eye in evolution*. Chicago: University of Chicago Press.

Edinger, T. (1929). Über knöcherne Scleralringe. *Zoologisches Jahrbuch, 51*, 164–226.

Ericson, P. G. P., Anderson, C. L., Britton, T., Elzanowski, A., Johansson, U., Källersjö, M., et al. (2006). Diversification of Neoaves: Integration of molecular sequence data and fossils. *Biology Letters, 2*(4), 543–547.

Felsenstein, J. (1985). Phylogenies and the comparative method. *The American Naturalist, 125*(1), 1–15.

Franz–Odendaal, T. A., & Hall, B. K. (2006). Skeletal elements within teleost eyes and a discussion of their homology. *Journal of Morphology, 267*(11), 1326–1337.

Friedmann, J. (1989). Regularized discriminant analysis. *Journal of the American Statistical Association, 84*(405), 165–175.

Garland, T., Jr., Harvey, P. H., & Ives, A. R. (1992). Procedures for the analysis of comparative data using phylogenetically independent contrasts. *Systematic Biology, 41*(1), 18–32.

Garland, T., Jr., Midford, P. E., & Ives, A. R. (1999). An introduction to phylogenetically based statistical methods, with a new method for confidence intervals on ancestral values. *American Zoologist, 39*(2), 374–388.

Grafen, A. (1989). The phylogenetic regression. *Philosophical Transactions of the Royal Society of London B, 326*(1233), 119–157.

Hackett, S. J., Kimball, R. T., Reddy, S., Bowie, R. C. K., Braun, E. L., Braun, M. J., et al. (2008). A phylogenomic study of birds reveals their evolutionary history. *Science, 320*(5884), 1763–1768.

Hall, M. I. (2008a). Comparative analysis of the size and shape of the lizard eye. *Zoology, 111*(1), 62–75.

Hall, M. I. (2008b). The anatomical relationships between the avian eye, orbit and sclerotic ring: Implications for inferring activity patterns in extinct birds. *Journal of Anatomy, 212*(6), 781–794.

Hall, M. I., & Ross, C. F. (2007). Eye shape and activity pattern in birds. *Journal of Zoology, 271*(4), 437–444.

Howland, H. C., Merola, S., & Basarab, J. R. (2004). The allometry and scaling of the size of vertebrate eyes. *Vision Research, 44*(17), 2043–2065.

Hughes, A. (1977). The topography of vision in mammals of contrasting life style: comparative optics and retinal organisation. In F. Crescitelli (Ed.), *The visual system in vertebrates* (pp. 613–756). Berlin, Heidelberg, New York: Springer–Verlag.

Kirk, E. C. (2004). Comparative morphology of the eye in primates. *Anatomical Record Part A, 281*(1), 1095–1103.

Kirk, E. C. (2006). Effects of activity pattern on eye size and orbital aperture size in primates. *Journal of Human Evolution, 51*(2), 159–170.

Land, M. F. (1981). Optics and vision in invertebrates. In M. F. Land, S. B. Laughlin, D. R. Nässel, N. J. Strausfeld, & T. H. Waterman (Eds.), *Comparative physiology and evolution of vision in invertebrates. B: Invertebrate visual centers and behavior I* (pp. 471–592). Berlin, Heidelberg, New York: Springer–Verlag.

Land, M. F., & Nilsson, D. E. (2002). *Animal eyes*. Oxford: Oxford University Press.

Leuckart, R. (1875). Organologie des auges. In A. Graefe & T. Saemisch (Eds.), *Handbuch der gesamten augenheilkunde, zweiter band, erste hälfte. anatomie und physiologie, zweiter theil, erste hälfte* (pp. 145–301). Leipzig: Verlag von Wilhelm Engelmann.

Lythgoe, J. N. (1979). *The ecology of vision*. Oxford: Clarendon Press.

Maddison, W. P., & Maddison, D. R. (2008). *Mesquite: a modular system for evolutionary analysis*. Version 2.5. <http://mesquiteproject.org>.

Marcot, J. D. (2007). Molecular phylogeny of terrestrial artiodactyls. In D. R. Prothero & S. E. Foss (Eds.), *Evolution of artiodactyls* (pp. 4–18). Baltimore: The Johns-Hopkins University Press.

Martin, G. R. (1982). An owl's eye: schematic optics and visual performance in *Strix aluco* L. *Journal of Comparative Physiology A, 145*(3), 341–349.

Martin, G. R. (1983). Schematic eye models in vertebrates. In D. Ottoson (Ed.). *Progress in sensory physiology* (Vol. 4, pp. 43–82). Berlin, Heidelberg, New York: Springer–Verlag.

Martin, G. R., Rojas, L. M., Ramirez, Y., & McNeil, R. (2004). The eyes of oilbirds (*Steatornis caripensis*): Pushing at the limits of sensitivity. *Naturwissenschaften, 91*(1), 26–29.

Mayr, G. (2005). The paleogene fossil record of birds in Europe. *Biological Reviews, 80*(4), 515–542.

McKenna, M. C., & Bell, S. K. (1997). *Classification of mammals above the species level*. New York: Columbia University Press.

Midford, P. E., Garland, T., Jr., Maddison, W. P. (2003). PDAP Package.

Motani, R., Rothschild, B. M., & Wahl, W. (1999). Large eyeballs in diving ichthyosaurs – The huge eyes of these extinct reptiles may have been useful deep in the ocean. *Nature, 402*(6763), 747.

Murphy, C. J., & Howland, H. C. (1987). The optics of comparative ophthalmoscopy. *Vision Research, 27*(4), 599–607.

Ott, M., & Schaeffel, F. (1995). A negatively powered lens in the chameleon. *Nature, 373*, 692–694.

Pereira, S. L., & Baker, A. J. (2006). A mitogenomic timescale for birds detects variable phylogenetic rates of molecular evolution and refutes the standard molecular clock. *Molecular Biology and Evolution, 23*(9), 1731–1740.

Pettigrew, J. D., Dreher, B., Hopkins, C. S., McCall, M. J., & Brown, M. (1988). Peak density and distribution of ganglion-cells in the retinae of microchiropteran bats – implications fro visual acuity. *Brain Behavior and Evolution, 32*(1), 39–56.

Prince, J. H. (1956). *Comparative anatomy of the eye*. Springfield: Charles C. Thomas.

Rencher, A. C. (2002). *Methods of multivariate statistics*. New York: John Wiley and Sons, Inc..

Ritland, S. (1982). *The allometry of the vertebrate eye*. PhD Thesis. Chicago: University of Chicago.

Ross, C. F. (2000). Into the light: The origin of the Anthropoidea. *Annual Reviews of Anthropology, 29*, 147–194.

Ross, C. F., & Kirk, E. C. (2007). Evolution of eye size and shape in primates. *Journal of Human Evolution, 52*(3), 294–313.

Schaeffel, F., & Wagner, H. (1996). Emmetropization and optical development of the eye of the barn owl (Tyto alba). *Journal of Comparative Physiology A: Neuroethology, Sensroy, Neural, and Behavioral Physiology, 178*(4), 491–498.

Schmitz, L. (2009). Quantitative estimates of visual performance features in fossil birds. *Journal of Morphology, 270*(6), 759–773.

Schulte, J. A., II., Valladares, J. P., & Larson, A. (2003). Phylogenetic relationships within the Iguanidae inferred using molecular and morphological data and a phylogenetic taxonomy of iguanian lizards. *Herpetologica, 59*(3), 399–419.

Slack, K. E., Jones, C. M., Ando, T., Harrison, G. L., Fordyce, R. E., Arnason, U., et al. (2006). Early penguin fossils, plus mitochondrial genomes, calibrate avian evolution. *Molecular Biology and Evolution, 23*(6), 1144–1155.

Tansley, K. (1965). *Vision in the vertebrates*. London: Chapman and Hall.

Thomas, R. J., Kelly, D. J., & Goodship, N. M. (2004). Eye design in birds and visual constraints on behaviour. *Ornitologia Neotropical, 15*, 243–250.

Thomas, R. J., Szekely, T., Cuthill, I. C., Harper, D. G. C., Newson, S. E., Frayling, T. D., et al. (2002). Eye size in birds and the timing of song at dawn. *Proceedings of the Royal Society London Series B, 269*(1493), 831–837.

Thomas, R. J., Szekely, T., Powell, R. F., & Cuthill, I. C. (2006). Eye size, foraging methods and the timing of foraging in shorebirds. *Functional Ecology, 20*(1), 157–165.

Vidal, N., & Hedges, S. B. (2005). The phylogeny of squamate reptiles (lizards, snakes, and amphisbaenians) inferred from nine nuclear protein-coding genes. *Comptes Rendus Biologies, 328*(10–11), 1000–1008.

Walls, G. L. (1942). *The vertebrate eye and its adaptive radiation*. New York: Hafner Pub. Co..

Warrant, E. (2004). Vision in the dimmest habitats on earth. *Journal of Comparative Physiology, A, 190*, 765–789.

Warrant, E. J. (2008). Nocturnal vision. In *The senses: A comprehensive reference*. In R. H. Masland & T. Albright (Eds.). *Vision II* (Vol. 2, pp. 53–86). Oxford: Academic Press.